

Anomalous Backward α Scattering

R. Stock*

Fachbereich Physik, Universität Marburg, Germany

and

G. Gaul and R. Santo

Sektion Physik, Universität München, Germany

and

M. Bernas,† B. Harvey, D. Hendrie, J. Mahoney, J. Sherman, J. Steyaert, and M. Zisman

Lawrence Radiation Laboratory, ‡ Berkeley, California 94720

(Received 26 June 1972)

The elastic α scattering to backward angles has been studied for $^{40,42,44,48}\text{Ca}$ between 40.7 and 72.3 MeV. The cross sections for ^{40}Ca are larger than those for the higher isotopes up to the highest energies. They show backward increases that disappear above 50 MeV. The enhancement factor for ^{40}Ca over $^{42,44}\text{Ca}$ varies smoothly with energy. ^{48}Ca does also show a backward cross-section enhancement over $^{42,44}\text{Ca}$. α -cluster rotational bands in the ^{44}Ti compound state, four-nucleon correlations in ^{40}Ca , and the l -dependent optical model are discussed as approaches to understand the anomaly. The rotator model appears to agree qualitatively with the experimental data. It involves rotational bands extending at least up to $J=16$ in ^{44}Ti .

1. INTRODUCTION

The elastic α scattering from the nuclei ^{40}Ca , ^{39}K , and ^{36}Ar has been termed anomalous because at angles beyond 90° the angular distributions do not decay with an exponential envelope typical for diffraction scattering.¹⁻³ The latter behavior is, however, found for the neighboring nuclei $^{42,44}\text{Ca}$, ^{41}K , and ^{40}Ar , as well as for all other nuclei above the s - d shell investigated hitherto, which are well described by a standard, four-parameter optical model.³⁻⁵ The anomaly consists of an enhancement of the backward cross section by up to 2 orders of magnitude. It has been observed at all incident energies investigated thus far, that is: between 18 and 42 MeV for ^{40}Ca and in the interval 18 to 30 MeV for ^{39}K and ^{36}Ar . A very pronounced oscillation is found in the enhanced cross-section domain, at all energies.

Numerous attempts have been made to reproduce these effects with a modified optical model. Acceptable fits to the α - ^{40}Ca scattering at 24 MeV were obtained⁵ by reducing the absorption in the surface region to about one third of its value in neighboring nuclei. However, different sets of parameters were necessary⁶ for values of the incident energy as close together as 4 MeV. Alternatively, a resonance term was introduced^{1,7} in the optical model for a partial wave close to the grazing angular momentum $l_0 = kR$. This procedure has been further investigated by McVoy.⁸ The average α scattering was described by a dif-

fraction model, to which a direct-channel Regge pole was added in order to account for the backward angle scattering. The interpretation given to the pole term was the formation of an α -cluster rotator structure in the compound system.⁸⁻¹⁰ Over a wide range of incident energies, the members of the corresponding "cluster rotational band" should dominate the backward scattering. The relative importance of such bands in neighboring compound systems such as ^{44}Ti and ^{48}Ti has not been investigated in terms of nuclear structure. Thus, this model cannot as of yet explain the isotope effect in α - $^{40,44}\text{Ca}$ scattering.

As an alternative explanation of anomalous α scattering, it has been proposed^{9,11} that the effect arises from an interaction of the incident α particle with correlated structures of four nucleons with $T=0$ in the target. It is known that ^{40}Ca has significant deformed $4p$ - $4h$ and $8p$ - $8h$ components, corresponding to two excited 0^+ states that mix into the ground state.¹² In these components the nucleons are not hindered by the Pauli principle from assuming a correlation that maximizes their mutual binding energy, whether their configuration is an " α cluster" with an intrinsic relative s state or, more generally a $T=0$ "quartet" structure.¹³ The p - h structure implies mostly excitation from the $d_{3/2}$ into the $f_{7/2}$ shell. If there are already neutrons present in the $f_{7/2}$ shell, they make the deformation less favorable, since they will occupy the lowest Nilsson orbits and block the $T=0$, $4p$ - $4h$ or $8p$ - $8h$ excitation mode. Such a blocking effect

may be responsible for the isotope effect in α scattering.³ The anomaly disappears in ^{40}Ar , ^{41}K , ^{42}Ca where there are always two $f_{7/2}$ neutrons present. The reaction mechanism by which correlations affect the elastic scattering has not been unambiguously settled. Most of the investigations use the cluster model, involving heavy-particle stripping,¹⁴ exchange plus knockout¹¹ or more general considerations of antisymmetrization¹⁵ as predominant contributions to the backward scattering.

Recently, the α -scattering data around $A = 40$ have been discussed in the framework of the l -dependent optical model.^{16,17} According to this model, the absorption is reduced for partial waves exceeding the maximum angular momentum L_c that can be carried away by the dominant exit channels. The (α, n) channel is considered most effective for the absorption. Because of the different thresholds for the (α, n) reaction, an explicit isotopic dependence is introduced in the optical model,

which is reflected in the different partial waves L_c at which the imaginary potential is cut off. The potential resulting for ^{40}Ca has a smaller absorption for the surface grazing partial waves than the average optical model. A good description of the 24-MeV α scattering from $^{40,42,44}\text{Ca}$, ^{41}K , and $^{36,40}\text{Ar}$ has been obtained.¹⁷

The aim of the present investigation was to study the backward α scattering at higher energies, choosing the Ca isotopes as targets because they appear most suitable for nuclear structure calculations. In particular, we wanted to answer the questions whether the anomaly disappears towards higher energies, and if this would indeed be observed, at which critical energy and in which way it ceases to exist. Such a characterization of the effect should play a decisive role in the matter of finding out the correct theoretical description from among the various models proposed to explain the anomaly. In the rotator model, a band cutoff would limit the effects at high angular mo-

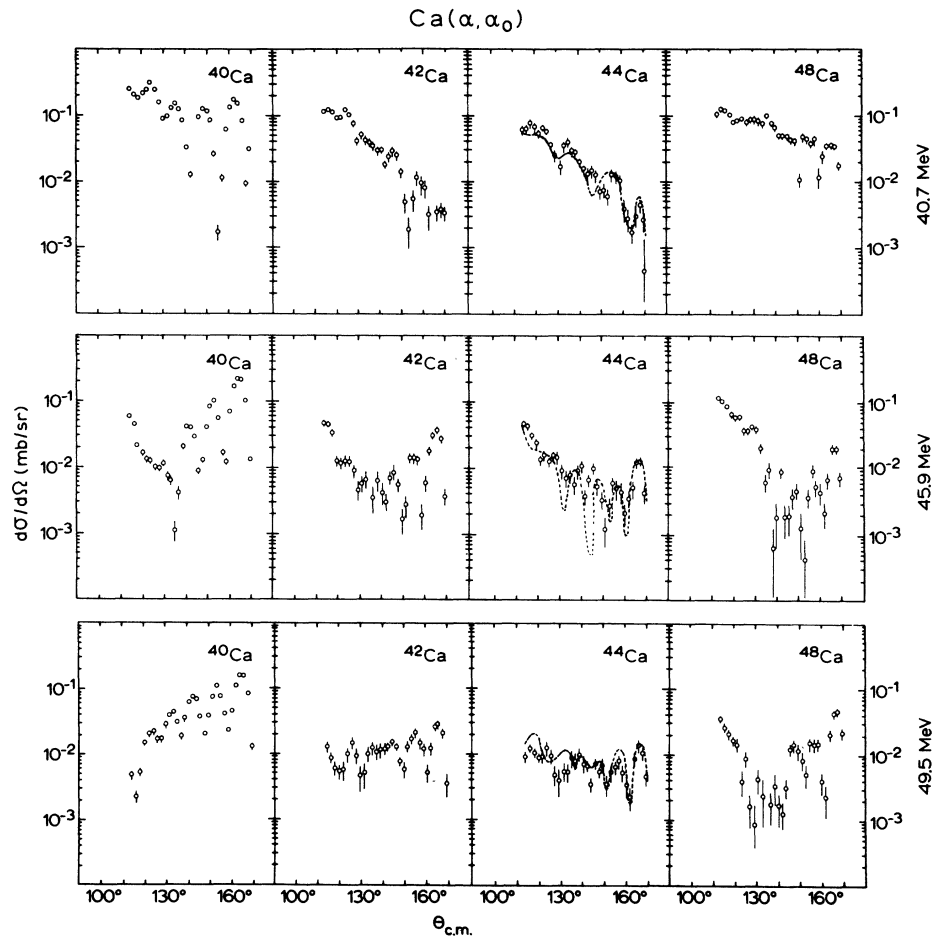


FIG. 1. Angular distributions for backward elastic α scattering from $^{40,42,44,48}\text{Ca}$ at 40.7, 45.9, and 49.5 MeV. The predictions of an energy-dependent optical model are shown for ^{44}Ca .

menta. Correlated structures can take momentum transfers only up to a certain maximum value. The l -dependent optical model, finally, predicts a maximal incident energy, beyond which the critical l value L_c is higher than the grazing momentum, and thus unobservable.¹⁶ Further, the behavior of α -⁴⁸Ca scattering at energies higher than 30 MeV was particularly interesting because at the highest energies investigated previously,³ ⁴⁸Ca shows an indication of backward enhancement and an angular distribution markedly different from ⁴²,⁴⁴Ca.

2. EXPERIMENTAL METHODS AND RESULTS

The backward elastic α scattering from ⁴⁰, ⁴², ⁴⁴, ⁴⁸Ca was measured at five energies between 40.7 and 72.3 MeV at the Berkeley 88-in. cyclotron. Eight solid-state detectors mounted in a scattering chamber were used. The targets contained a mixture of the four calcium isotopes, except for the maximum energy runs where unmixed targets were used. The metallic targets were self-supporting, of about 600- $\mu\text{g}/\text{cm}^2$ thickness. They were transferred into the chamber under dry argon to prevent oxidation. The thickness was determined by weighing a 1- cm^2 area of the targets used in the experiments. The isotopic composition was measured by mass spectrometric analysis with an accuracy better than 2%. The same mixed target was used for the runs at 40.7, 45.9, 49.5, and 65.6 MeV. Over the angular range from 110 to 170° in the lab system, the

different recoil-energy loss permitted the separation of the four elastic reactions. The target abundance of 55% in ⁴⁰Ca, 15% in ⁴²Ca, 17% in ⁴⁴Ca, and 12% in ⁴⁸Ca, led sometimes to rather poor statistics for ⁴², ⁴⁴, ⁴⁸Ca, the cross sections being in the 1- to 10- $\mu\text{b}/\text{sr}$ range.

The angular distributions for the four isotopes of Ca and five incident energies are shown in Figs. 1 and 2. The most significant features of the results are:

- (1) While there are backward increases for ⁴⁰Ca, as well as a variety of other angular distribution shapes for the other isotopes up to 49.5 MeV, there are no significant differences in the angular distributions above 50 MeV: All distributions decay exponentially.
- (2) A very pronounced oscillatory structure is observed for ⁴⁰Ca up to 50 MeV which is washed out at higher energy.
- (3) The ⁴⁰Ca cross sections are enhanced over the other isotopes at all energies.
- (4) The angular distributions and absolute cross sections for ⁴²Ca and ⁴⁴Ca are very similar, with ⁴²Ca showing somewhat higher backward cross sections below 65.6 MeV.
- (5) ⁴⁸Ca shows higher absolute cross sections than ⁴², ⁴⁴Ca at all energies. It also shows backward peaking and pronounced oscillations, although different from ⁴⁰Ca, at 45.9 and 49.5 MeV. In the following analysis, we want to concentrate on ⁴⁰Ca and ⁴⁴Ca. We take the results of Ref. 3 for 18-, 22-, 24-, and 29-MeV incident energy into consideration simultaneously with the present data.

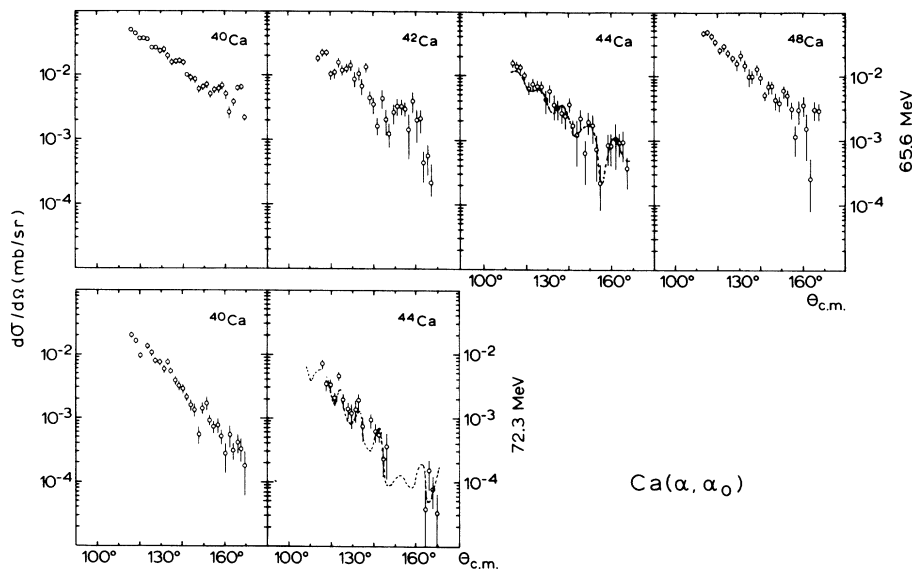


FIG. 2. Angular distributions and optical-model fits for α scattering at 65.6 and 72.3 MeV.

Then we observe, for energies up to 50 MeV and angles from 110 to 170° , the following correlation between ^{40}Ca and ^{44}Ca : (i) If the ^{44}Ca cross section falls with an exponential envelope ^{40}Ca stays approximately constant (18, 29, and 40.7 MeV); (ii) if the ^{44}Ca envelope shows a minimum at about 130° , so does ^{40}Ca but with a much steeper increase from 130° to the very backward angles (22 and 45.9 MeV); (iii) if, finally, the ^{44}Ca cross-section envelope is approximately horizontal, ^{40}Ca rises exponentially (24 and 49.5 MeV).

Thus, the shape of the backward angular distribution as a whole appears to fluctuate with the incident energy, for *both* isotopes, with ^{40}Ca always showing an enhancement over ^{44}Ca and a more pronounced oscillatory pattern. Above 50 MeV, the oscillations of ^{40}Ca are damped and similar to ^{44}Ca . The angular distribution shapes are similar, too, but ^{40}Ca is still enhanced. From data obtained for α - ^{40}Ca scattering at 104 MeV, it is clear that there is no backward increase reappearing at higher energies¹⁸; no isotope studies have been carried out.

To further illustrate the ^{40}Ca enhancement, we show in Fig. 3 the backward cross sections, integrated for $117^\circ \leq \theta_{\text{c.m.}} \leq 169^\circ$, for $^{40,44}\text{Ca}$. The data of Ref. 3 are included. Both excitation functions show a largely similar structure. The enhancement of ^{40}Ca decreases from 1 order of magnitude at low energies to a factor of about 5 at 72 MeV. The enhancement factor itself varies very smoothly with energy.

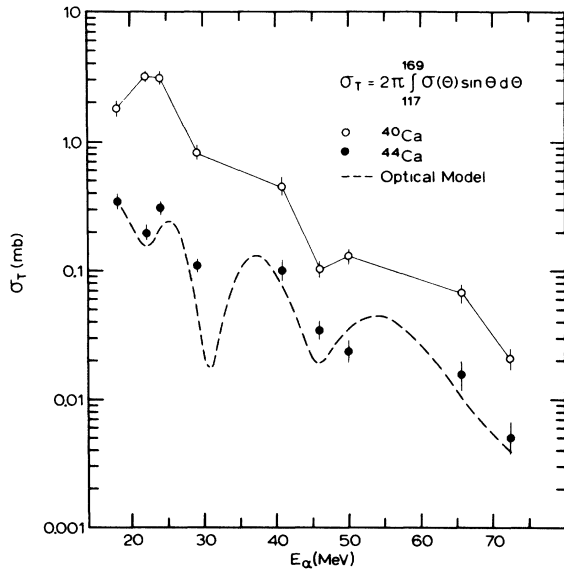


FIG. 3. Integrated backward-angle cross sections for elastic α scattering from ^{40}Ca and ^{44}Ca . The optical-model excitation function for ^{44}Ca is given as a dashed line; the solid line is drawn to guide the eye.

3. OPTICAL-MODEL ANALYSIS

From previous investigations it is known that the α - ^{44}Ca scattering below 30 MeV can be very well described by the standard optical model.^{3,4} Applied to ^{40}Ca , it always underestimates the backward cross sections but gives a correct fit to the forward angles up to the third diffraction maximum. This latter angular region of optical model calculations is much more sensitive against the geometry (and to some extent the depth) of the real than of the imaginary part of the potential.

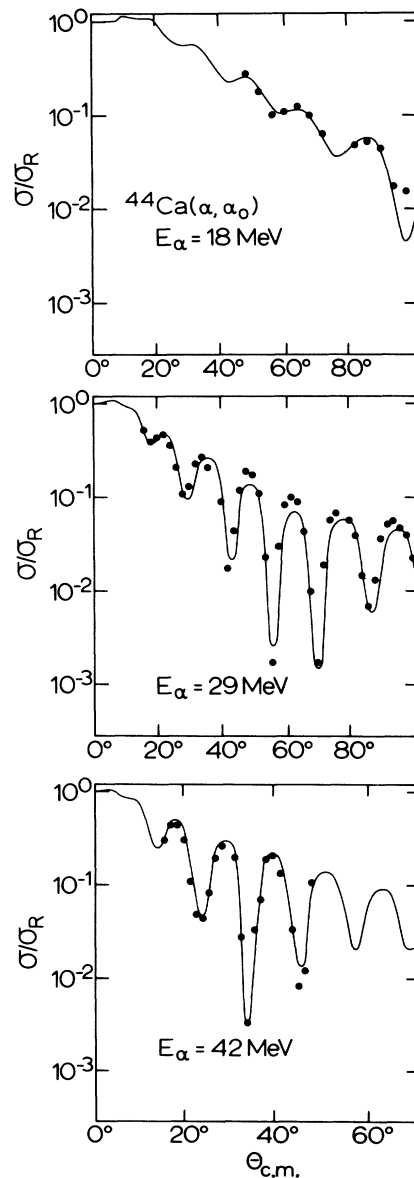


FIG. 4. Fit to forward-angle α scattering from ^{44}Ca at 18 and 29 MeV (Ref. 3), and 42 MeV (Ref. 20) with the energy-dependent optical model.

Thus, there seems to exist a real potential common to ^{40}Ca and ^{44}Ca forward scattering, the backward differences reflecting mostly an isotope effect on the absorption. In order to describe this difference in terms of the optical model it was necessary to extend the standard optical model up to 70-MeV incident energy.

In the optical-model calculations for ^{44}Ca over the whole range of energies available, an energy dependence of the α -scattering potential had to be taken into account.¹⁹ With the fixed set of parameters ($V=183.7$ MeV, $W_{\text{vol}}=26.6$ MeV, $r_v=r_w=1.4$ fm, $a_v=a_w=0.564$ fm) that described the average elastic scattering⁴ from nuclei between ^{44}Ca and ^{50}Ti below 30 MeV, the ^{44}Ca backward cross sections are overestimated by more than 1 order of magnitude at higher energies. Our backward-angle data turned out to be particularly sensitive to the energy dependence of the imaginary part. Starting from the above set of parameters an extensive grid search was performed where only the imaginary depth and radius were varied with energy. It was not intended to obtain best fits at individual energies but rather to reproduce the predominant features of the angular distributions over the whole range of energies. The forward angles were included in the search between 18 and 29 MeV and at 42 MeV, where data of Fernandez and Blair²⁰ are available. The resulting energy dependence can be approximated by

$$\begin{aligned} W(E) &= 14.3 + 0.42E_{\alpha}, \\ r_w &= 1.43 - 2.8 \times 10^{-3}E_{\alpha} + 5.4 \times 10^{-5}E_{\alpha}^2. \end{aligned} \quad (1)$$

The fits obtained for the forward angles at 18, 29, and 42 MeV are shown in Fig. 4. The fits to the present ^{44}Ca data are given in Figs. 1 and 2. With the inclusion of the energy dependence in the imaginary potential it is thus possible to define a standard potential that describes the whole range of incident energies.

The calculated excitation function for the integrated backward cross section from ^{44}Ca is also shown in Fig. 3. It is in fair agreement with the data, although more experimental points would be necessary to determine whether the peak to valley ratios of the gross fluctuations with energy are physical. The minima at 30 and 46 and the point of inflection at about 65 MeV correspond to surface grazing partial waves $l_0=13$, 17, and 21. However, these structures cannot be attributed to partial-wave resonances with the corresponding l_0 values. Rather, they are caused by a superposition of a few neighboring partial waves as can be shown by letting W go to zero, whereupon the broad maxima split up into a sequence of resonances with widths of about 1 MeV.

No systematic fit was attempted to the ^{40}Ca data. At individual energies, the backward enhancement could be parametrized by a drastic reduction of the absorption.

4. SUMMARY AND DISCUSSION

Summarizing the above results we may say that the anomaly in backward α scattering from ^{40}Ca consists of a $\frac{1}{2}$ - to 1-order-of-magnitude enhancement in the integrated cross sections over those from $^{42,44}\text{Ca}$ and the energy-dependent standard optical model. The enhancement shows a very slow variation with incident energy. Below 50 MeV, it takes the form of a backward-peaked scattering amplitude added to the average. But there is a similar enhancement in the absence of any backward peaking, at energies above 50 MeV. The nucleus ^{48}Ca does also show an enhanced integrated cross section at all energies, and more pronounced oscillatory angular distributions than $^{42,44}\text{Ca}$ at 45.9 and 49.5 MeV.

The implication of these results with respect to the theoretical models outlined in the Introduction will be discussed in the following paragraphs.

A. Rotator Model

According to McVoy,⁸ the α -scattering amplitude $S_{(l)}^E$ for a given energy E may be expressed as

$$S(l) = B(l) \left[1 + i \frac{D(l)}{l - L - i\Gamma(l)/2} \right], \quad (2)$$

where $B(l)$ describes the background, nonresonant scattering and may be calculated from a diffraction or standard optical model. The Wigner term in l space describes a resonance, centered at L , with elastic width $D(l)$ and total width $\Gamma(l)$. With varying energies the resonances occur at energies $E_{n,L}$, where n is the main quantum number and L the α rotator angular momentum. The index n labels a rotational band comprising a set of L values.

Let us first consider the dependence on l for fixed energy. In the case of a small $\Gamma(l)$, i.e., for a $\Gamma(l)$ not larger than 1 unit of \hbar , the resonant amplitude will be dominated by a single l value, L . The backward cross section then takes the form of $|P_L(\cos\theta)|^2$, weighted by $|D(L)/\Gamma(L)|^2$. Fits to the backward angular distributions by single $|P_L|^2$ are shown in Fig. 5 for energies between 22 and 49.5 MeV. The phase of the oscillation is fairly well reproduced, at all energies.

Calculations with the full scattering amplitude as given by Eq. (2) were performed at 24 and 49.5 MeV. The background amplitude $B(l)$ was taken from the average optical-model potential for ^{44}Ca as described in Sec. 3. The results are shown in

Fig. 6 which also gives the parameters obtained from the search. It turns out that $D \sim \frac{1}{2}\Gamma$ and $\Gamma \lesssim \hbar$ for both energies. Further the calculations indicate that the quality of the fits depends sensitively not only on the ratio of D and Γ , but on the absolute value of either of these quantities.

In the absence of a resonance [vanishing $D(l)$] or in the case of a large overlap of adjacent resonances [large $\Gamma(l)$], the backward cross section would appear rather structureless. We observe such angular distributions at 65 and 72 MeV, for all Ca isotopes.

With respect to the sequence of L poles observed at various incident energies, Cowley and Heymann¹⁰ as well as Rinat⁹ have observed that they should form a rotational band, with a moment of inertia as given by the α -target grazing configuration. In Fig. 7 we show a plot of $L(L+1)$ versus the energy in the compound system ^{44}Ti , for all energies where we find an angular distribution of reasonably pure $|P_L|^2$ type. Within the experimental uncertainty resulting from the random selection of incident energies, the points may indeed be connected by a straight line. The extrapolated excitation energy of the $L=0$ "band head" is at about 10 MeV in ^{44}Ti . The solid line represents the values of $l_0(l_0+1)$, where l_0 is the classical grazing angular momentum ($|\eta_{l_0}| \sim \frac{1}{2}$). We observe that the resonances L occur at angular momenta smaller than

l_0 , at all energies. This, and the location of the band head well above the ^{44}Ti ground state, may indicate either an excitation of the target core in the resonance or the formation of a rotational band with a main quantum number higher than zero. In the first case, the resonances would have to be interpreted as doorway states, whereas in the latter case, one would describe them as a sequence of shape resonances with $n=1$. In either case, the rotator model appears to reproduce the dominant features of the anomalous α - ^{40}Ca scattering.

The isotope effect could in this model be explained²¹ by a dependence on nuclear structure of either or both of the quantities D and Γ . Since $D(l)$ is proportional to a "reduced α width" of the compound resonance at $E_{n,l}$, the simplest way to account for a vanishing of the anomaly would be a small α width. In the case of the Ca targets, this should happen for ^{44}Ca where the many degrees of freedom of the $f_{7/2}$ 4 neutron configuration couple to the $\alpha + ^{44}\text{Ca}$ core configuration. At the ^{40}Ca and ^{48}Ca shell closures there are only rather inert groups of nucleons present in the target, favoring a rotator. This simple picture would qualitatively match our data. The disappearance of the ^{40}Ca backward increase above 50 MeV, along with the washing out of the oscillations, indicates an increase of $\Gamma(l)$ towards higher energies and a corresponding phase averaging among various adja-

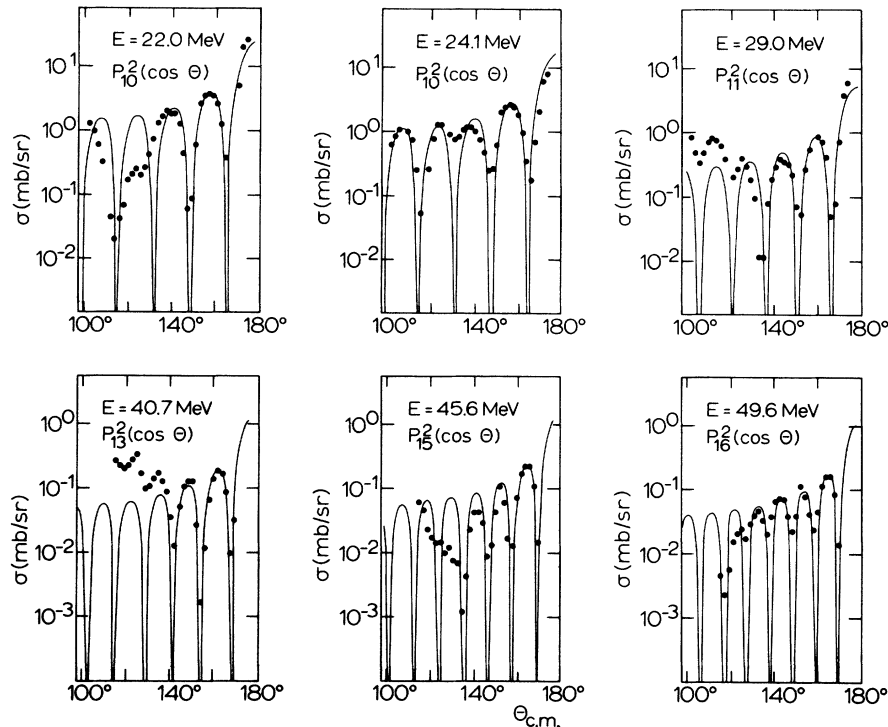


FIG. 5. Fits to the backward α scattering from ^{40}Ca by the square of a single Legendre polynomial $P_L(\cos\theta)$.

cent P_l , for all isotopes. Still, $D(l)$ must be larger for $^{40,48}\text{Ca}$ than for ^{44}Ca in order to account for the cross-section enhancement over ^{44}Ca .

B. Target Correlations

Instead of discussing the detailed mechanism by which four-nucleon correlations with $T=0$ in the target ground state could result in a backward scattering enhancement,^{11,14} we want to base the discussion on a consideration of the momentum transfer in backward scattering.

For intermediate angles in the backward region, the α -scattering momentum transfer q equals about 650 MeV/c at 25 MeV, and 1150 MeV/c at 75 MeV. This momentum has to be absorbed by target nucleons which can, at most, take twice the Fermi momentum $q_F \sim 270$ MeV/c. Thus, above 25 MeV the backward scattering requires an interaction with more than one nucleon. This means that the path length the projectile has to pass in order to dissipate its momentum increases with energy. On it the projectile is subjected to the absorption into nonelastic channels. With increasing energy, backward elastic scattering

becomes more unlikely and the angular distribution decays more rapidly with angle. However, if there would be groups of correlated nucleons present in the target, scattering from such groups could dissipate more momentum in each event, resulting in a shorter pathlength than with uncorrelated nucleons. Backward scattering from a correlated target could therefore be enhanced at a given energy. This general argument applies to all reaction mechanisms like heavy particle stripping or α exchange that involve four-nucleon $T=0$ substructures in the target. They do all favor high-momentum transfer and lead to enhanced backward scattering.

Both the cluster²² and the more general quartet¹³ models predict a correlation in space or, at least in the angular orientation of a $T=0$ group of four nucleons. In the elastic scattering from the intrinsic s -state "cluster component" of such a structure, the maximum possible momentum transfer should be approximately four times larger than for independent nucleons.

Indeed, if we in a very primitive model calculate the cluster state as an α particle bound in a Woods-Saxon potential, we obtain a real well depth of 140 MeV for ^{40}Ca . This would give the weakly bound cluster a momentum of approximately 900 MeV/c. One would then predict an enhancement of backward α - ^{40}Ca scattering up to incident energies beyond 100 MeV. As our data show, the enhancement factor of ^{40}Ca over ^{44}Ca is still 5 at 72.3 MeV.

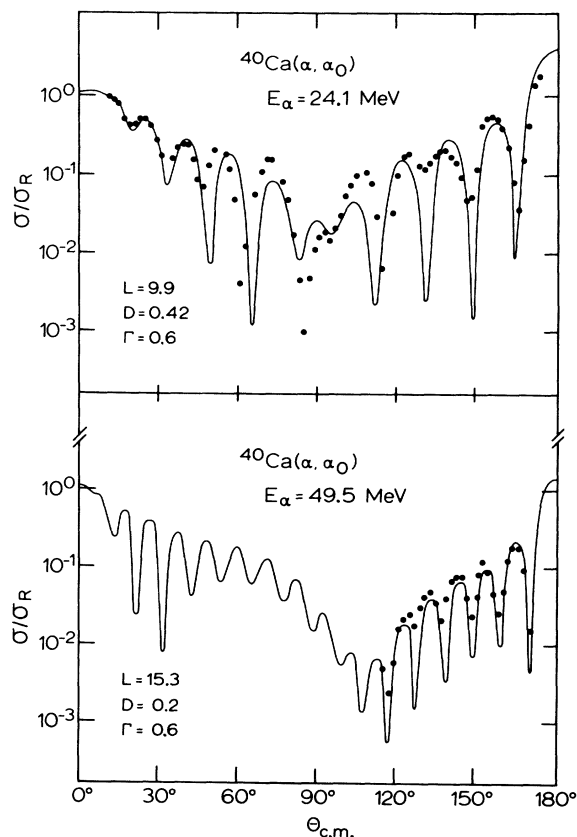


FIG. 6. Optical-model-plus-Regge-pole calculations for α - ^{40}Ca scattering at 24 and 49.5 MeV.

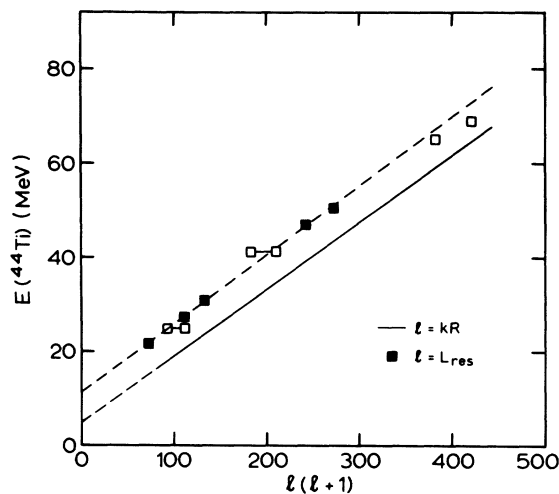


FIG. 7. Rotational band formed by the resonant angular momenta L of backward α - ^{40}Ca scattering. The plot gives $L(L+1)$ versus the excitation energy in the compound system ^{44}Ti . Ambiguous L assignments are indicated. The band-head energy is about 10 MeV. The full line represents $l_0(l_0+1)$ for the grazing angular momentum l_0 .

In this model one would thus assume that ^{40}Ca has α -cluster components in its ground state that are reduced or entirely absent in ^{44}Ca but appear again in ^{48}Ca . A critical test of this prediction has recently been attempted by Zafiratos *et al.*²³ They compared the α pickup cross sections from the targets ^{40}Ca and ^{40}Ar by means of the (^3He , ^7Be) reaction. Substituting ^{40}Ar for ^{44}Ca as a target does not impair the test because these two nuclei show almost identical, normal α scattering at all energies investigated thus far.³ Zafiratos *et al.* observe the same α -particle spectroscopic factors for ^{40}Ca and ^{40}Ar in the transitions to the ground and first excited 2^+ levels of ^{36}Ar and ^{36}S , respectively. However, this result is not conclusive for the nonexistence of a significant cluster component in ^{40}Ca . According to the quartet model¹³ the $T=0$, relative s -state cluster component in a 0^+ ground state is not coupled to the minimal core spins 0^+ and 2^+ , but rather to high-spin states like 6^+ and 8^+ . The four nucleons of a quartet have a vanishing s -state component if they are coupled to the 0^+ core. The selection rules for the (^3He , ^7Be) reaction allow only for s -state pickup. Thus, the observed transition strengths are due to other than the quartet components in the ^{40}Ca and ^{40}Ar ground states, leaving the question of α correlations in ^{40}Ca still open.

C. l -Dependent Optical Model

In the general formulation of the l -dependent optical model,¹⁶ the absorption of the surface partial waves around $l_0 = kR$ is taken to be proportional to the density of energy conserving reaction channels available to carry away l_0 units of angular momentum. The density depends on the structure of the target. At shell closures, $W(l_0)$ is reduced leading to a backward enhancement of the cross section and to strong oscillations.¹⁷

If the optical-model amplitude is parametrized by the expression (2) the l -dependent model appears as a special case of the rotator model. The real part of the optical model determines $D(l)$ and the positions $E_{n,l}$ of the resonancelike states. The imaginary part appears in the total width $\Gamma(l)$. A reduction of W for partial waves around l_0 implies a small $\Gamma(l_0)$ which leads to anomalous scattering, provided $D(l)$ is not too small. The statement of the l -dependent optical model would therefore be that only $\Gamma(l)$ – and not $D(l)$ – is dependent on the target structure.

The dependence of W on the specific nuclear structure should disappear towards higher energies¹⁶ rendering $\Gamma(l)$ equal for ^{40}Ca and ^{44}Ca as targets. The energy where this should happen has not yet been calculated. It appears unlikely, how-

ever, that much of the structural dependence is left at compound-nuclear excitations above 50 MeV, where a multitude of channels such as $(\alpha, 2\alpha)$, $(\alpha, 2n)$, etc., is open. Thus, at 65 and 72 MeV of incident energy, $\Gamma(^{40}\text{Ca}) \sim \Gamma(^{44}\text{Ca})$. This would be consistent with the similarity of the angular distributions of ^{40}Ca and ^{44}Ca , but leaves the ^{40}Ca enhancement unexplained, calling for a structural dependence of $D(l)$. This question can only be finally answered by a consistent analysis of angular distributions taken over a wide range of energies in steps of about 1 MeV. However, data for the complete angular range from about 20° to 170° would be required to make an analysis unambiguous. Such data are not yet available above 30 MeV. An analysis of data at lower energy is in progress.²⁴

The present data do, however, indicate that it is not appropriate to consider the (α, n) channel alone representative for the optical-model absorption, as suggested by Eberhardt.¹⁷ From the (α, n) thresholds, one would obtain a reduction of W for ^{40}Ca which disappears towards ^{44}Ca and is entirely absent in ^{48}Ca . However, ^{48}Ca does also show contributions of anomalous backward scattering. The cutoff in the imaginary part must therefore be more sensitively dependent on the specific nature and the degrees of freedom of the neutron excess than it is expressed in the (α, n) thresholds.

5. CONCLUSIONS

The elastic backward α scattering from the Ca isotopes deviates from predictions of the standard optical model both in its drastic dependence on the target isotope and in the variation with energy in the shape of the angular distributions obtained for ^{40}Ca scattering. These effects exhibit a certain similarity to the observations made in heavy-ion scattering. In the elastic scattering of ^{16}O from ^{16}O , a structure is observed in the excitation function that cannot be accounted for by a simple-minded optical model.²⁵ Further, the ^{16}O - ^{18}O scattering²⁶ shows a distinctly different behavior, indicating a pronounced isotope dependence. Both the heavy-ion and the α -scattering processes are governed by a high angular-momentum input and by a large momentum transfer. In that respect, α backward scattering may provide insight into the still more complex situation with colliding heavy ions where the concept of an optical-model potential is of very hypothetical nature. The importance of the anomalies is not restricted to elastic scattering. It extends to all reactions with channels where such phenomena occur and which, nevertheless, are frequently analyzed in the framework of a direct reaction mechanism.

The models that have been proposed to explain the backward α scattering effects appear to be in qualitative agreement with the observations. The assumption of an interaction of the projectile with specific "cluster" structures in the target could explain the deviation from standard optical-model scattering at high momentum transfer. The rotator model ascribes the effects to orbiting states in the compound system. The l -dependent optical model should, in its most general form, provide insight into the dependence on the target structure of the width parameters entering the rotator model. The predicted sequence of resonances that behaves like a rotational band is in agreement with

the experimental data. Still, the question has to be answered whether these resonances are shape resonances or involve a target excitation, which would then suggest to characterize them as doorway states. More experimental data and an extensive theoretical analysis are required to clarify this question.

M. Bernas and R. Stock would like to thank B. Harvey for making a very fruitful stay at the Lawrence Radiation Laboratory, Berkeley, possible. We thank Dr. M. Michel for the isotopic analysis of the targets. We are most grateful to H. Fuchs, J. Hüfner, and A. Richter for many stimulating discussions.

*On leave of absence from Max-Planck-Institut für Kernphysik, Heidelberg, Germany.

†Permanent address: Institut de Physique Nucléaire, Orsay, France.

‡Work supported in part by the U. S. Atomic Energy Commission.

¹C. R. Gruhn and N. S. Wall, Nucl. Phys. **81**, 161 (1966).

²A. Bobrowska, A. Budzanowski, G. Grotowski, L. Jarczyk, L. Micek, H. Niewodniczanski, A. Strzalkowski, and Z. Wrobel, Nucl. Phys. **A126**, 361 (1969).

³G. Gaul, H. Lüdecke, R. Santo, H. Schmeing, and R. Stock, Nucl. Phys. **A137**, 177 (1969).

⁴R. Bock, P. David, H. H. Duhm, H. Hefele, U. Lynen, and R. Stock, Nucl. Phys. **A92**, 539 (1967).

⁵L. McFadden and G. R. Satchler, Nucl. Phys. **84**, 177 (1966).

⁶H. Lüdecke, Ph.D. thesis, Heidelberg, 1969 (unpublished).

⁷A. Budzanowski, A. Dudek, R. Dymartz, K. Grabowski, L. Jarczyk, H. Niewodniczanski, and A. Strzalkowski, Nucl. Phys. **A126**, 369 (1969).

⁸K. W. McVoy, Phys. Rev. C **3**, 1104 (1971).

⁹A. S. Rinat, Phys. Letters **38B**, 281 (1972).

¹⁰A. A. Cowley and G. Heymann, Nucl. Phys. **A146**, 465 (1970).

¹¹N. C. Schmeing, Nucl. Phys. **A142**, 449 (1970).

¹²W. J. Gerace and A. M. Green, Nucl. Phys. **A123**, 241 (1969).

¹³A. Arima and V. Gillet, in *de-Shalit Memorial Volume* (Annals of Physics, 1971).

¹⁴J. Noble and H. Coelho, Phys. Rev. C **3**, 1840 (1971).

¹⁵G. W. Greenlees and Y. C. Tang, Phys. Letters **34B**, 359 (1971).

¹⁶R. A. Chatwin, J. S. Eck, D. Robson, and A. Richter, Phys. Rev. C **1**, 795 (1969).

¹⁷K. A. Eberhardt, Phys. Letters **33B**, 343 (1970).

¹⁸Karlsruhe cyclotron group, private communication by M. Rebel.

¹⁹H. Schmeing, Ph.D. thesis, Heidelberg, 1970 (unpublished).

²⁰B. Fernandez and J. S. Blair, Phys. Rev. C **1**, 523 (1970).

²¹H. Oeschler, H. Schröter, H. Fuchs, L. Baum, G. Gaul, H. Lüdecke, R. Santo, and R. Stock, Phys. Rev. Letters **28**, 694 (1972).

²²V. G. Neudachin and Yu. F. Smirnov, At. Energy Rev. **3**, 157 (1965).

²³C. D. Zafiratos, C. Dètraz, C. E. Moss, and C. S. Zaidins, Phys. Rev. Letters **27**, 437 (1971).

²⁴G. Gaul, H. Fuchs, H. Oeschler, R. Santo, and R. Stock, to be published.

²⁵J. V. Maher, M. W. Sachs, R. H. Siemssen, A. Weidinger, and D. H. Bromley, Phys. Rev. **188**, 1665 (1969).

²⁶R. W. Shaw, R. Vandenbosch, and M. K. Mehta, Phys. Rev. Letters **25**, 457 (1970); R. H. Siemssen, H. T. Fortune, A. Richter, and J. W. Tippie, to be published.